Chemical Engineering Journal 451 (2023) 138685

Contents lists available at ScienceDirect

Chemical Engineering Journal

journal homepage: www.elsevier.com/locate/cej

Polyamide microplastics act as carriers for cephalexin in the anammox process

Ye Wang, Dong-Qi Huang, Jun-Hui Yang, Gui-Feng Li, Ye-Xing Zhou, Jia-Yi Zhang, Ya Lu, Nian-Si Fan [*,1], Ren-Cun Jin [*,2]

Laboratory of Water Pollution Remediation, School of Life and Environmental Sciences, Hangzhou Normal University, Hangzhou 311121, China

A R T I C L E I N F O

Keywords:
Anammox
Polyamide microplastics
Cephalexin
Adsorption
Oxidative stress

A B S T R A C T

Emerging pollutants pose high risks to human health, and also put huge pressures on wastewater treatment. Their interactions would also affect the activity of functional microorganisms. This study investigated the response and mechanism of anaerobic ammonium oxidation (anammox) consortia to the long-term stress of common microplastics (polyamide, PA) and a broad-spectrum antibiotic (cephalexin, CFX). Although 0.1 g L^{-1} PA microplastics (MP) did not significantly inhibit the nitrogen removal performance, adsorption assays revealed that large amounts of cephalexin were adsorbed by PA. Thus, 0.5 mg L^{-1} CFX and 0.1–0.2 g L^{-1} PA caused a deterioration of anammox process. Simultaneously, the most dominant genus changed from *Candidatus* Kuenenia to *norank o SBR1031*, and expressional levels of functional genes dramatically decreased. In addition, the abundance of gene encoding superoxide dismutase (SOD) increased by 10.7 %, verifying that PA also caused the oxidative stress of anammox bacteria. PA promoted the accumulation of CFX in the anammox system through adsorption and extended its side effects on anammox consortia. This study provides a new direction into the implementation of anammox process in complex wastewater treatment.

1. Introduction

The urbanization development leads to the increase of water consumption worldwide, raising huge pressures on wastewater treatment [1]. The effective treatment of nitrogen-containing wastewater is one of the most important goals [2]. At present, several denitrification processes have been widely studied, such as partial nitrification–denitrification (PND), simultaneous nitrification–denitrification (SND) and anaerobic ammonium oxidation (anammox). The former two processes could simplify reaction and save space, respectively [3,4]. Anammox process is an autotrophic nitrogen removal process without adding exogenous carbon sources. It is an emerging biotechnology with the advantages of high nitrogen loading rate and low energy consumption [5]. However, anammox bacteria are susceptible to environmental changes, such as pH, temperature, light and various pollutants [6,7], which limits the extensive application of anammox process. Recently, emerging pollutants become a research hotspot in wastewater treatment, among which antibiotics have drawn public attention due to their threats to human health [8]. Moreover, high-concentration antibiotics induce abundant antibiotic resistance genes (ARGs), which have also been recognized as emerging pollutants [9]. Different antibiotics exhibited different effects on the anammox granules. Previous studies reported that the anammox process were inhibited by 50 mg L^{-1} norfloxacin and oxytetracycline [10,11], while it could tolerate amoxicillin, florfenicol and sulfamethazine with the concentrations of 60 mg L^{-1}, 10 mg L^{-1} and 100 mg L^{-1}, respectively [12]. As one of the most widely used antibiotics, cephalexin (CFX) has a broad antibacterial spectrum and is highly effective against anaerobic bacteria [13]. Concentrations of CFX ranged from ng L^{-1} to μg L^{-1} in natural waters, and it was frequently detected at the mg L^{-1} level in wastewater treatment plants [14,15]. Previous studies reported that CFX potentially reduced granular stability in aerobic granular sludge [15]. Meng, et al. [16] found that CFX inhibited the process performance of expanded granular sludge bed, especially the soluble chemical oxygen demand removal, and this inhibition was reversible. However, whether the fate and effect of CFX in anammox system are similar remains unclear.

* Corresponding authors.
E-mail addresses: fns1907@163.com (N.-S. Fan), jrczju@aliyun.com (R.-C. Jin).
[1] ORCID: 0000-0001-8640-8223.
[2] ORCID: 0000-0002-1337-7531.

https://doi.org/10.1016/j.cej.2022.138685
Received 16 May 2022; Received in revised form 1 August 2022; Accepted 16 August 2022
Available online 18 August 2022

As another hot spot of current researches, MPs have been widely detected in wastewaters, such as polyamide (PA), polyethylene and polyethylene terephthalate [17,18]. MPs can enter cells and lead to the disorders of microbial physiological functions, including digestion, reproduction and respiratory capacity [19,20]. Tang, et al. [21] found that 0.5 g L^{-1} polyvinyl chloride reduced the average ammonia nitrogen removal rate from 93.3 % to 87.1 % in anammox process. Furthermore, MPs could induce oxidative stress. Hydrolysis of waste activated sludge was inhibited by the oxidative stress caused by polyethylene terephthalate [22]. The co-occurrence of antibiotics and MPs may have synergetic or antagonistic effect. For example, the nitrification performance was not affected by 0.5 mg L^{-1} triclosan, while the co-occurrence of polyvinyl chloride, triclosan and polyvinyl chloride led to the reactor malfunction rapidly [23]. Polyamide 6 (PA 6) could promote the production of methane during anaerobic digestion, due to the caprolactam released by PA 6 [24]. In the partial nitrification system, PA reduced the diversity of microbial communities and promoted the transfer of ARGs [25].

Due to their low degradability and hydrophobicity, MPs can transport the absorbed contaminants, which allow MPs to be better carriers for hydrophobic organic compounds [17,26]. Polychlorinated bisphenyls (PCBs) in MPs were 10^5-10^6 times higher than that in the surrounding seawater [27,28]. The potential adsorption between MPs and emerging pollutants may cause serious environmental concerns due to the changes in their environmental fate, bioavailability and biomagnification [29]. Previous studies on the co-occurrence of antibiotics and MPs showed that their effects on biological reactors may be synergistic. For example, 0.5 mg L^{-1} triclosan did not affect the nitrification performance, while triclosan and PVC could quickly lead to the reactor malfunction [23]. The combined toxicity of PA and sertraline also reduced the NRE of activated sludge process and the abundance of denitrifying bacteria [30]. However, these studies mainly discussed the performance of anaerobic digestion, nitrification, partial nitrification and corresponding microbial community shift. As common emerging pollutants, the influence of coexist and mechanism of MPs and antibiotics on anammox process remain unknown. PA is widely used in clothing textile, medical textile and automobile manufacturing [31,32]. As one of the most common MPs in wastewater, few studies have been reported on the PA influences in wastewater treatment process, especially the anammox process [33]. Therefore, this study objective is to systemically evaluate the comprehensive effects of PA and CFX on the anammox process performance, exhibit the response of anammox consortia to the long-term stress of PA and CFX, and elucidate the interaction mechanism among PA, CFX and microorganisms in the anammox system.

2. Materials and methods

2.1. Seed sludge and reactors set up

The inoculated sludge was collected from a laboratory-scale upflow anaerobic sludge bed (UASB) reactor which had been stably operated for 5 years with the SAA and VSS of 13.6 ± 5.6 mg N g^{-1} VSS h^{-1} and 2.9 ± 0.2 g L^{-1}, respectively. The dominant anammox bacteria was *Candidatus* Kuenenia. Two reactors (R_0 and R_1) with an effective volume of 1.5 L were constructed. The 0.5 L anammox granules were inoculated to each reactor with the initial sludge biomass of 2.7 ± 0.1 g L^{-1}.

2.2. Operational strategy

In this study, PA and CFX (purity of 98 %) were purchased from McLean Biochemical Technology Co., Ltd. (Shanghai, China). The particle size of PA ranged from 37 to 75 μm. The influent substances in forms of $(NH_4)_2SO_2$ and $NaNO_2$ were purchased from Sinopharm Chemical Reagent Co., Ltd. (Beijing, China). In order to avoid excessive NO_2^--N, the ratio of ΔNO_2^--N/ΔNH_4^+-N was 1:1. In addition, inorganic salt solutions and trace elements were also added to the synthetic wastewater. The specific components and concentrations of inorganic salt solution were listed in Table S1. Both UASB reactors were operated at 35 ± 1 °C with a hydraulic retention time (HRT) of 1.71 h. The duration of continuous flow experiment was 300 d, which was divided into five phases (Table S2). In P0, 0.1 g L^{-1} PA was added to R_1 to determine the single impact of PA on the anammox system. In P1, 0.1 g L^{-1} PA and 0.5 mg L^{-1} CFX were added to evaluate their combined effects on the system. In P2, increasing the PA concentration (0.2 g L^{-1}) was to verify whether PA could promote or alleviate the inhibition of CFX. In P3, further increasing the concentration of CFX (1 mg L^{-1}) was to investigate whether the tolerance of the system to high concentration CFX increased after long-term tolerance to 0.5 mg L^{-1} CFX. In the last phase, whether the reactor could recover to the initial level and corresponding strategies were explored.

2.3. Collection and characterization of samples

The specific experimental procedure is shown in Fig. S1. The concentration of NH_4^+, NO_2^- and NO_3^- were determined using spectrophotometric methods. At the end of each phase, specific anammox activity (SAA) was determined by calculating consumption rate of nitrite via batch assays. At the end of P0-P3, 10 mL sludge samples were collected from the reactor after gently mixing and temporarily stored at −20 ℃ for subsequent experiments. High performance liquid chromatography (HPLC, Shimadzu, Japan) was used to determine CFX concentrations, and the recovery was 101.5 %. PS and PN contents in EPS were measured using the anthrone method and modified Lowry method, using glucose and bovine serum albumin (BSA) as standard, respectively. A fluorescence spectrophotometer (EEM, Hitachi, Japan) was used to collect the fluorescence spectrum of EPS, and a Fourier transform infrared (FTIR) spectrometer (Thermo Fisher, USA) was used to characterize the chemical bonds of EPS. Morphologies of anammox sludge and PA were observed via a scanning electron microscopy (SEM, Zeiss, Germany).

2.4. Gene quantification and microbial community analysis

DNA and RNA were extracted by a Power Soil DNA Kit (MoBio Laboratories, USA) and Power Soil RNA Isolation Kit (MoBio Laboratories, USA), respectively. This study assayed functional genes (*hdh*, *hzs*A and *nir*S), ARGs (bla_{TEM} and bla_Z), *int*I1 and the oxygen detoxification related gene (SOD) by quantitative PCR (qPCR). The expression level of *hdh*, *hzs*A and *nir*S were further quantified by reverse transcription qPCR (RT-qPCR). The primers and annealing temperatures are listed in Table S3. High-throughput sequencing (HTS) was conducted on the Illumina MiSeq platform by Majorbio (Shanghai, China). Raw sequencing data were deposited in NCBI-SRA database under the accession number SRR 18683159-68.

2.5. Batch adsorption experiment

Batch experiments intended to determine the adsorption ability of MPs and sludge for CFX. Four concentrations (i.e., 0.5, 1, 5, 10 and 15 mg L^{-1}) of CFX and 0.1 g L^{-1} PA were mixed in 100 mL foil-wrapped serum bottles and incubated at 35 °C and 180 rpm for 1810 min. The adsorption between 0.1 g L^{-1} PA and 1 g anammox sludge were also detected similarly. The mixtures were filtered through filters (0.22 μm) to remove PA and further analyzed using HPLC. The amount of CFX adsorbed onto PA was calculated using the mass balance method as described in Supplementary Materials. Pseudo-first-order kinetics (PFO) and pseudo-second-order kinetics (PSO) were adopted to fit the adsorption kinetics of CFX, and the details were given in Supplementary Materials.

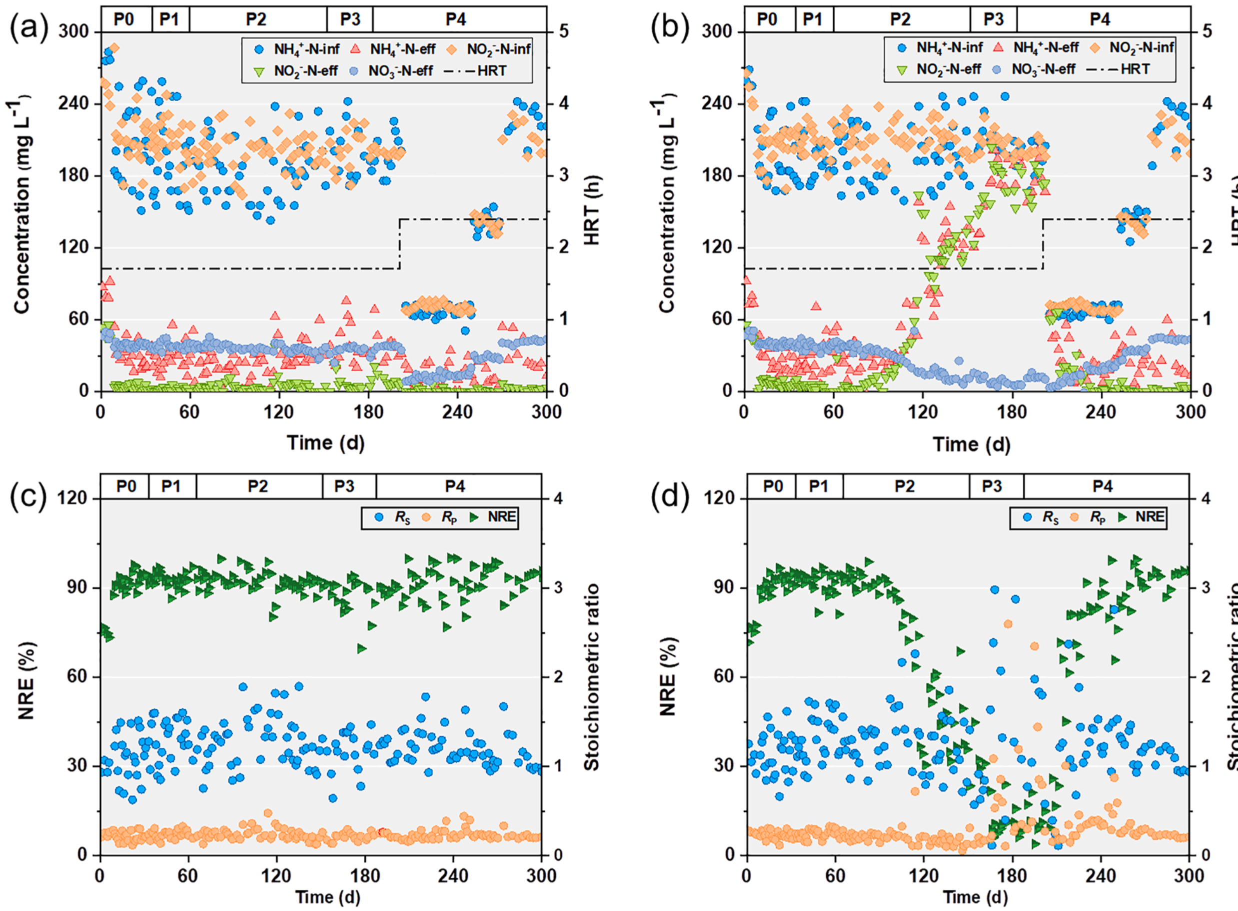

Fig. 1. Nitrogen removal performance of R_0 (a and c) and R_1 (b and d) during the whole period. NRE: nitrogen removal efficiency.

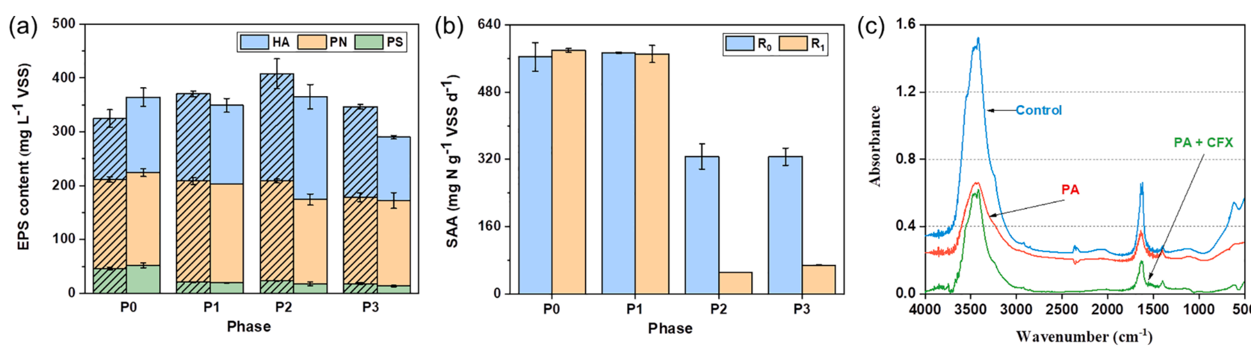

Fig. 2. Extraction of extracellular polymer (EPS): R_0 (with shadow) and R_1. Specific anammox activity (SAA) in R_0 and R_1 (b). FTIR absorbance spectra of the EPS sample (c).

3. Result and discussion

3.1. Nitrogen removal performance

All reactors were stabilized for 11 days, and the nitrogen removal efficiency (NRE) and nitrogen removal rate (NRR) were 90.0 ± 0.7 % and 5.9 ± 0.3 kg N m^{-3} d^{-1}, respectively (Fig. 1 and S2). The SAA was 579.2 mg N g^{-1} VSS d^{-1} at the end of P0 (Fig. 2). The stoichiometric molar ratio of R_S (ΔNO_2^--N/ΔNH_4^+-N) and R_P (ΔNO_3^--N/ΔNH_4^+-N) in R_0 and R_1 approximated the theoretical values of 1.32 and 0.26, respectively. Under the stress of 0.1 g L^{-1} PA in P1, the NRE of R_1 remained stable at 92.5 ± 3.2 %, which might be attributed to the protection of EPS [23]. Polyethylene (0.1 wt%) could change the substrate availability and promote the NH_4^+ oxidation and NO_3^- reduction rates of anammox process in freshwater sediments [34]. When R_1 was exposed to 0.1 g L^{-1} PA and 0.5 mg L^{-1} CFX at the beginning of P2 (61–95 d), the nitrogen loading rate (NLR), NRR and NRE were approximately 5.8 ± 0.5 kg N m^{-3} d^{-1}, 5.3 ± 0.5 kg N m^{-3} d^{-1} and 92.3 ± 3.54 %, respectively. Afterwards, the complex of CFX and PA was deposited and accumulated in anammox granular sludge. NRR and NRE sharply dropped to 2.0 kg N m^{-3} d^{-1} and 35.8 % on day 96, respectively. High-concentration of both pollutants could induce bacterial death by inhibiting the synthesis of cell walls, which further caused the process deterioration [35–37].

In P3, NRE and NRR of R_1 continued to decline to 11.4 % and 0.6 kg N m^{-3} d^{-1}, respectively. To evaluate the reversibility, PA and CFX were no longer fed in P4. No recovery trend was observed until day 201, with the NRE of 16.2 ± 10.2 %. Therefore, the influent total nitrogen

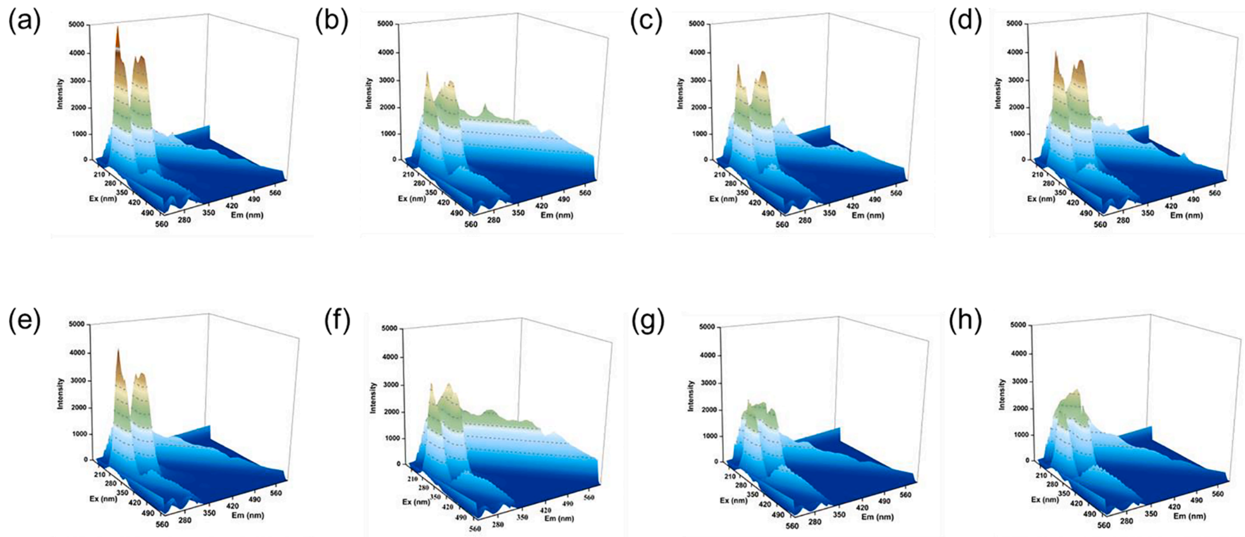

Fig. 3. 3D-EEM fluorescence spectra of EPS in R_0 (P0-3: a–d) and R_1 (P0-3: e–h).

concentrations were reduced to 140 mg L^{-1}, and HRT was adjusted to 2.4 h. After 73 days, the NRE of R_1 gradually increased to 86.0 %. The influent substrate concentrations gradiently increased to 420 mg L^{-1}. NRR simultaneously increased to 4.0 kg N m^{-3} d^{-1}, and NRE maintained at 93.7 ± 3.0 %. Although the side effects of CFX and PA on the anammox process were relatively persistent, the performance could be recovered with the strategy of substrate and HRT adjustment.

3.2. Changes in anammox granular property

In comparison, the EPS content in R_0 remained relatively stable (Fig. 2), which was consistent with the granular morphology observed by SEM (Fig. S3). In P1 and P2, the EPS content gradually increased to 365.6 mg g^{-1} VSS. EPS is essential for the bacterial resistance to pollutant stress, and is regarded are the “demarcation zone” between surrounding environment and bacteria [38]. Zhang, Zhang, Wei, Huang, Wang, Wang and Ni [18] also reported that polyethylene terephthalate induced EPS production in anaerobic granular sludge systems. In P3, the EPS content decreased to 290.1 mg g^{-1} VSS, because antibiotics thwarted the formation of peptide bonds and further reduced PN synthesis [39]. The fluorescence peaks of EEM spectra of two reactors at different phases exhibited two obvious peaks (Fig. 3). Peak A (Ex/Em: 225/300–310) and Peak B (Ex/Em: 275/335–340) had been reported to be protein-like substances or tyrosine [40–42] and tryptophan substances [43], respectively. In R_1, peak A and B intensities in P1 did not change significantly but decreased significantly in P2, indicating that CFX and PA inhibited the secretion of protein-like and tryptophan substances.

The functional groups of EPS were characterized by FTIR spectroscopy (Fig. 2). Three peaks were detected at 621 cm^{-1}, 1637 cm^{-1} and 3452 cm^{-1}, corresponding to the γN-H in protein of fingerprint region, beta sheet structure of protein secondary structure and the stretching vibration of the hydroxyl bond, respectively [44–46]. Hydroxyl content is closely related to the hydrophilicity of granules. Reduction of hydroxyl content in R_1 represented the increase of anammox granular hydrophobicity. However, 0.5 g L^{-1} polybutylene succinate was reported to enhance the hydrophilicity of anammox sludge [21]. The PA-caused increase of PN was mainly responsible for such difference.

3.3. Fate and adsorption of CFX in anammox system

The influent concentrations of CFX in P2 and P3 were 0.474 mg L^{-1} and 0.436 mg L^{-1}, respectively. The pre-adsorption of MPs in the influent might be responsible for the discrepancy between the measured and theoretical (0.5 mg L^{-1}) values. In P2, the effluent concentration of CFX still maintained a high value of 0.424 mg L^{-1}, while it dramatically decreased to 0.18 mg L^{-1} in P3. The increasing concentrations of PA in P3 probably adsorbed more CFX and detained them in the anammox system. Batch assays showed that the adsorption of antibiotics on anammox sludge was negligible in this system (Fig. 4). Previous studies have proven that oxygen-containing functional groups are generated on MP surface when they are hydrolyzed or biodegraded, leading to a decrease in the MP hydrophobicity and an increase in the adsorption of β-lactam antibiotics [47,48]. According to the adsorption kinetics of CFX on PA, the adsorption rate continuously slowed and reached the equilibrium finally (Fig. 4). Moreover, the adsorption curves of CFX were more fitted to PFO model, except for the CFX concentration of 0.5 mg

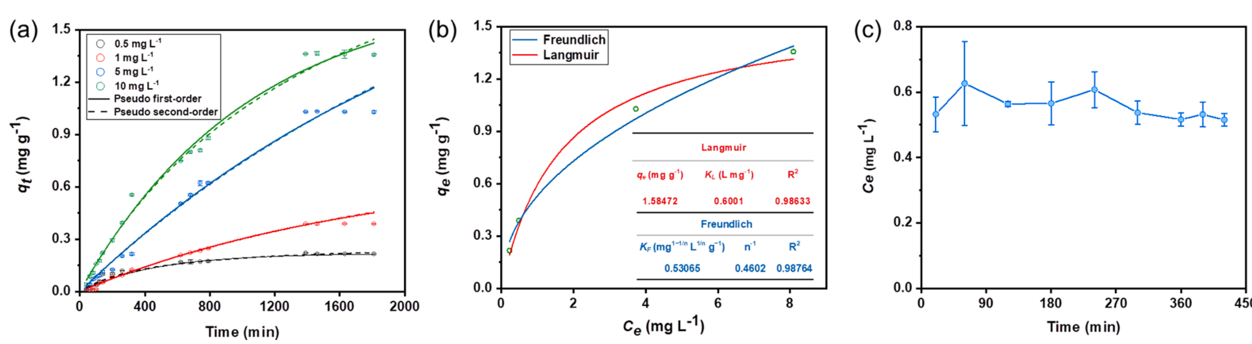

Fig. 4. Adsorption kinetics (a) and adsorption isotherms of different concentrations of CFX on PA (b). Adsorption of CFX on anammox granules (c).

Table 1
Fitting parameters of PA to CFX adsorption kinetics.

PA-MP Conc.[a] (g L^{-1})	CFX Conc. (mg L^{-1})	Pseudo first-order				Pseudo second-order			
		$q_{e, cal}$ (mg g^{-1})	$q_{e, exp}$ (mg g^{-1})	k (h^{-1})	R^2	$q_{e, cal}$ (mg g^{-1})	$q_{e, exp}$ (mg g^{-1})	k (mg g^{-1} h^{-1})	R^2
0.1	0.5	0.21807	0.21635	0.00215	0.9692	0.28174	0.21635	0.00754	0.9732
0.1	1	0.72006	0.38883	0.00055	0.9945	1.23564	0.38883	0.00026	0.9941
0.1	5	2.29168	1.02856	0.00039	0.9927	4.20882	1.02856	0.00051	0.9919
0.1	10	1.73133	1.35732	0.00096	0.9945	2.73854	1.35732	0.00023	0.9938

[a] PA: polyamide microplastics; Conc.: Concentration.

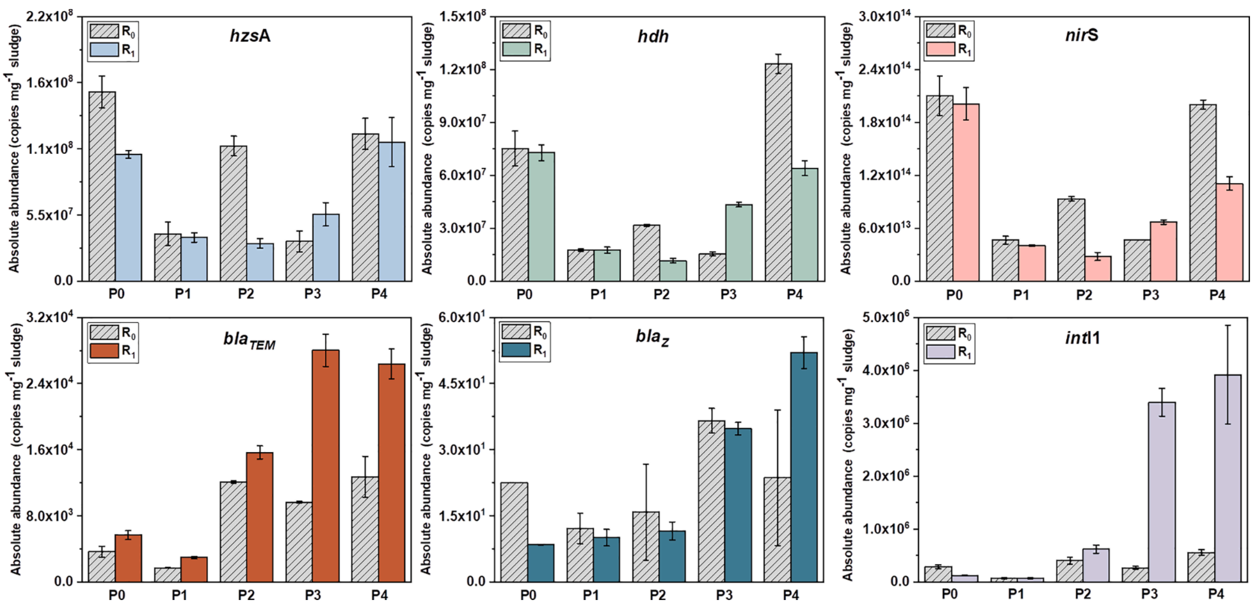

Fig. 5. Absolute abundances of functional genes and ARGs.

L^{-1} (Table 1). The experimental adsorption capacity (q_{cal}) was closer to the actual value (q_{exp}) in the PFO model. Wagstaff, Lawton and Petrie [17] also proposed that three cationic drugs (propranolol, amitriptyline, and fluoxetine) onto PA was well-fitted by the PSO model. The discrepancy in data fitting might be due to physical adsorption and chemical adsorption existed simultaneously in the process of polyamide adsorption of cephalexin. Polarity is another factor affecting the ability of MPs to adsorb chemicals [49]. The adsorption isotherm of PA was nonlinear. The Freundlich model fitted the data well ($R^2 = 0.9876$), suggesting that the interaction between CFX and PA was multilayer adsorption due to surface nonuniformity. It was also indirectly proved that PA had multiple adsorption sites and active groups [50]. The maximum adsorption capacity of PA was higher than that of the other five MPs, which also fit the Freundlich isotherm model [51]. The strength of adsorption was usually related to the constant n [52]. In this study, n^{-1} was less than 1, indicating that the adsorption capacity of PA decreased with CFX concentration. In general, the antibiotic removal of anammox system largely depended on the MPs adsorption.

3.4. Variations in key functional genes and ARGs

Changes in the abundances of three functional genes (*hzs*A, *nir*S and *hdh*) were similar (Fig. 5). In P0 and P1, there was no significant difference between R_0 and R_1. In P2, the abundances of in R_1 were decreased from 3.6×10^7, 1.8×10^7 and 4.0×10^{13} copies mg^{-1} sludge to 3.1×10^7, 1.2×10^7 and 2.8×10^7 copies mg^{-1} sludge, which were significantly less than those in R_0 of 1.1×10^8, 3.2×10^7 and 9.3×10^7 copies mg^{-1} sludge, respectively. In P3, the abundances of *hzs*A, *hdh* and *nir*S in R_1 began to rebound, which was irreconcilable with the reactor performance and the anammox bacteria abundance described above. Although abundances of three functional genes increased, their expressional levels remained low based on the RT-qPCR results (Fig. S5). During the recovery phase, both expressional level and the abundance of *hzs*A, *hdh* and *nir*S were recovered. The accumulation of antibiotics in biological systems promote the horizontal transfer of ARGs through mobile genetic elements (MGE). The integron encoding gene *int*I1 is a common indicator for evaluating the potential gene transfer ability [53]. The abundance of *int*I1 in R_1 increased significantly from 7.3×10^4 to 3.4×10^6 copies mg^{-1} sludge in P1-P3, verifying that the main driving force of ARG transfer was antibiotic stress. Simultaneously, the abundance of bla_{TEM} also increased, especially in P3.

3.5. Microbial responses to CFX and PA pressures

Microbial community analysis revealed that Shannon index of R_1 generally increased, indicating that the addition of PA and CFX increased the bacterial diversity in the anammox system (Table S4). ACE and Chao index of R_1 were increased initially and then decreased from P3, suggesting that high-concentration MPs reduced the population richness. In addition, redundancy analysis (RDA) at the OTU level showed that the microbial community structure significantly changed under CFX stress (Fig. 6). Although the nitrogen removal performance of R_1 recovered in P4, the microbial community structure remained different from that of R_0, implying the persistent effect of CFX and PA.

Planctomycetes, Proteobacteria, and Chloroflexi were the dominant phyla in these systems (Fig. S6). The relative abundance of Chloroflexi in R_1 showed a significantly increased from 20.8 % to 30.39 % in P2, suggesting that 0.5 mg L^{-1} CFX mainly contributed to the increase in Chloroflexi abundance. Chloroflexi could utilize EPS secreted by anammox bacteria as substrate [54], which explained the reductions in

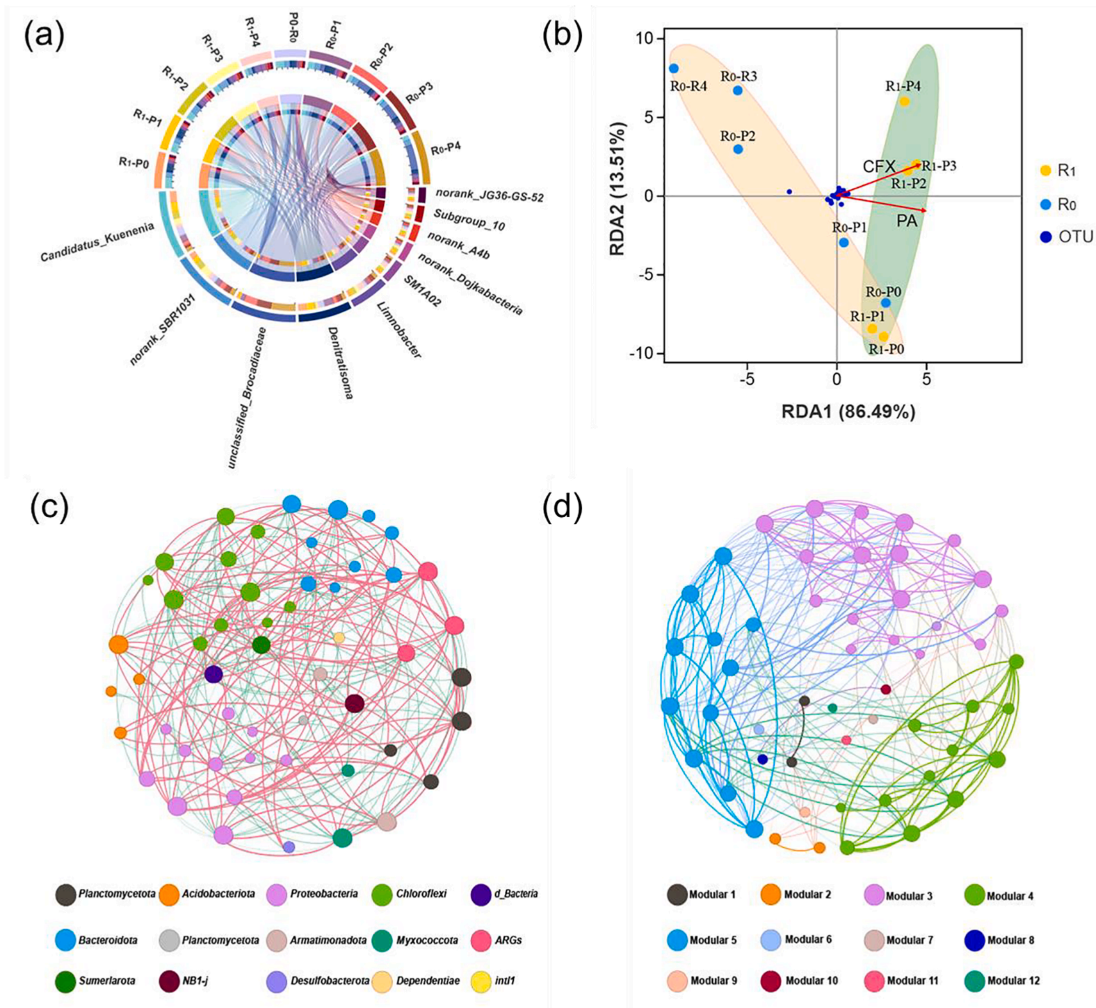

Fig. 6. Dominant microbial community in anammox systems at the genus level (a) and redundancy analysis of microbial community at the OTU level (b). *Norank* and *unclassified* indicate unclear taxonomic status at the genus level. Network analysis colored by the phylum level (c) and modularity class (d).

EPS in P2 and P3. The abundance of Planctomycetes, which the anammox bacteria belonging to, was comparatively stable initially. After the addition of CFX, its abundance decreased dramatically decreased to 16.2 % at the end of P3, which corresponded to the nitrogen removal performance. Similar phenomenon was also observed in the anammox system stressed by PA66-MP Zhao, et al. [55]. The accumulation of antibiotic-microplastic complex probably exacerbated the bacterial inactivity or death. The most dominant genus in R_1 was *Candidatus* Kuenenia in P1 with the abundance of 20.3 ± 0.02 %, and then it changed to *norank_o_SBR1031* from P2 to the end (16.5 ± 1.6 %). The *norank_o_SBR1031* had been widely detected in anammox systems, but its specific function was unclear [56]. Denitrifying bacteria were also detected in this system, such as *Thermomonas*, *Dokdonella*, *Denitratisoma* and *Pseudomonas* [57]. In addition, the abundances of *Thermomonas* and *Pseudomonas* gradually increased during the experimental period, indicating they might participate in the nitrogen removal process especially under antibiotic stress. It is worth noting that *Candidatus* Kuenenia was replaced by *unclassified*_Brocadiaceae as the main anammox bacteria in R_0 during the stabilization period. The dominant anammox bacteria species would change in different feast-famine states [58]; thus, the microbial succession in this system was mainly caused by the transient reduction of nitrogen load from 700 mg L^{-1} to 420 mg L^{-1}.

Correlation analysis revealed that *int*I1 and ARGs (bla_{TEM} and bla_Z) were significantly positively correlated (Fig. S4). The relationship between ARGs (bla_Z and bla_{TEM}), *int*I1 and microbial communities was analyzed by network modulation (Fig. 6). Populations with similar niches are classified as a functional unit in bacterial community, which can also be regarded as a module [59]. The network generated 12 modules, and the nodes were derived from 13 phyla. In terms of the dominant (top 49) genera, there were two anammox bacteria *Candidatus* Kuenenia and *unclassified*_Brocadiaceae in this system. *Candidatus* Kuenenia was closely related to *Bryobacter* and *Limibaculum*. Anaerobic bacteria frequently coexist with heterotrophic bacteria to tolerate harsh environments [60]. *Unclassified*_Brocadiaceae was positively correlated with *Ignavibacterium*. In addition, bla_{TEM} and bla_Z were positively correlated with *Ardenticatenales*, *SWB02* and *NB1.j*, indicating that these microorganisms were the potential hosts of these β-lactam ARGs.

3.6. Mechanism of anammox process responding to antibiotic and MPs

MPs mainly affect the abundance and activity of functional bacteria, and further change the substrate availability in anammox process [34,61]. In this study, the single effect of 0.1 g L^{-1} PA on the anammox process performance was not significant. However, CFX was adsorbed and accumulated by MPs, which inhibited the activity of anammox bacteria severely. The abundant channels and pores on the surface of PA, which provide sufficient adsorption sites for various pollutants (Fig. S3). The adsorption process of CFX and PA was better fitted with the PSO model, suggesting that it was mainly chemical adsorption. PA had a contact angle of 107.7°, PA confirming its hydrophobicity [62]. CFX was

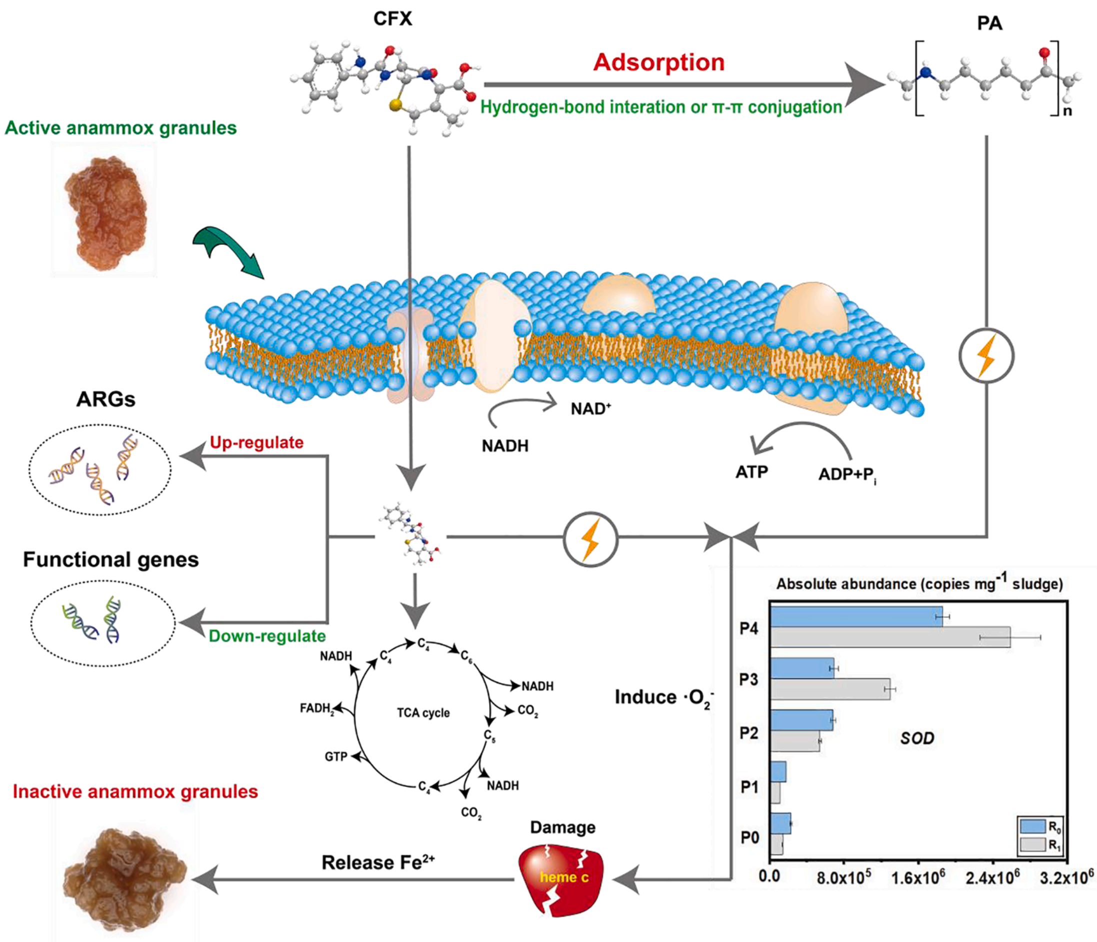

Fig. 7. The proposed influence process in anammox bacteria induced by PA and CFX.

an amphoteric molecule, indicating that it could bind with PA through hydrophobic interactions [63]. It had been proved that oxygen-containing functional groups played a crucial role in adsorption process, and π-π conjugation and hydrogen bond were also the potential forms of the adsorption process [64–66]. The N—H stretching and amide carbonyl promote the hydrogen bonding interaction between EDC and PA [67]. On the other hand, antibiotics were continuously accumulated in the anammox reactor via adsorbing on MPs. High-concentration antibiotics not only induced ARGs transfer but also disturbed the tricarboxylic acid (TCA) cycle, which further promoted the production of reactive oxygen species (ROS) and the destruction of heme *c* [68]. SOD is involved in the removal of superoxide anion radical $\bullet O_2^-$, which is a type of ROS [69]. The abundance of gene *SOD* in R_0 and R_1 was similar during P0 and P1, while it in R_1 dramatically increased to 1.3×10^6 copies mg^{-1} sludge in P3 (Fig. 7). Therefore, high-concentration PA was the main force of oxidative stress. SOD could convert $\bullet O_2^-$ into H_2O_2, which also caused the cell death in the anammox system [70,71]. However, the removal strategy of the MPs and antibiotics deposited in the system remains to be further developed.

4. Conclusion

The addition of low-concentration PA exhibited no significant effect on the nitrogen removal performance, but high concentrations of PA caused the oxidative stress. Due to the adsorption of CFX by PA, MPs functioned as antibiotic carriers in the anammox process. The accumulation and inhibition of CFX on anammox consortia were extended, resulting in the performance deterioration of anammox process. In the recovery phase, such inhibition could be artificially relieved through adjusting influent substrate concentrations and HRT. The reversible of anammox system to CFX and PA was mainly attributed to ARGs accumulation and microbial community succession during the 300-d domestication. The predominant bacteria changed from *Candidatus* Kuenenia to *norank_o_SBR1031*. This study elucidates the co-effect and interaction mechanism of PA and CFX in the anammox system, and further provides a new idea for the implementation of anammox technology to treat wastewater containing various pollutants.

Declaration of Competing Interest

The authors declare that they have no known competing financial interests or personal relationships that could have appeared to influence the work reported in this paper.

Data availability

Data will be made available on request.

Acknowledgement

The authors are grateful for financial support from the Science and Technology Development Program of Hangzhou (20201203B123) and the National Natural Science Foundation of China (52000055).

Appendix A. Supplementary data

Supplementary data to this article can be found online at https://doi.org/10.1016/j.cej.2022.138685.

References

[1] X. Zheng, W. Zhou, R. Wan, J. Luo, S.u. Yinglong, H. Huang, Y. Chen, Increasing municipal wastewater BNR by using the preferred carbon source derived from kitchen wastewater to enhance phosphorus uptake and short-cut nitrification-denitrification, Chem. Eng. J. 344 (2018) 556–564.

[2] S. Cao, D.u. Rui, Y. Peng, B. Li, S. Wang, Novel two stage partial denitrification (PD)-Anammox process for tertiary nitrogen removal from low carbon/nitrogen (C/N) municipal sewage, Chem. Eng. J. 362 (2019) 107–115.

[3] D.u. Rui, S. Cao, B. Li, M. Niu, S. Wang, Y. Peng, Performance and microbial community analysis of a novel DEAMOX based on partial-denitrification and anammox treating ammonia and nitrate wastewaters, Water Res. 108 (2017) 46–56.

[4] Q. Wang, J. He, Complete nitrogen removal via simultaneous nitrification and denitrification by a novel phosphate accumulating Thauera sp. strain SND5, Water Res. 185 (2020), 116300.

[5] X. Rui, B.-J. Ni, S. Liu, L.u. Huijie, Impacts of organics on the microbial ecology of wastewater anammox processes: Recent advances and meta-analysis, Water Res. 191 (2021), 116817.

[6] M. Tomaszewski, G. Cema, A. Ziembińska-Buczyńska, Significance of pH control in anammox process performance at low temperature, Chemosphere 185 (2017) 439–444.

[7] D.-Q. Huang, J.-J. Fu, Z.-Y. Li, N.-S. Fan, R.-C. Jin, Inhibition of wastewater pollutants on the anammox process: A review, Sci. Total Environ. 803 (2022) 150009.

[8] Z. Bi, G.e. Song, X. Sun, Deciphering antibiotic resistance genes and microbial community of anammox consortia under sulfadiazine and chlortetracycline stress, Ecotoxicol. Environ. Saf. 234 (2022), 113343.

[9] Y.-r. Chen, X.-P. Guo, Z.-S. Niu, D.-P. Lu, X.-l. Sun, S. Zhao, L.-J. Hou, M. Liu, Y. i. Yang, Antibiotic resistance genes (ARGs) and their associated environmental factors in the Yangtze Estuary, China: From inlet to outlet, Mar. Pollut. Bull. 158 (2020) 111360.

[10] G.-F. Yang, Q.-Q. Zhang, R.-C. Jin, Changes in the nitrogen removal performance and the properties of granular sludge in an Anammox system under oxytetracycline (OTC) stress, Bioresour. Technol. 129 (2013) 65–71.

[11] X. Zhang, Z. Chen, Y. Ma, N. Zhang, D. Wei, H. Zhang, H. Zhang, Response of partial nitrification sludge to the single and combined stress of CuO nanoparticles and sulfamethoxazole antibiotic on microbial activity, community and resistance genes, Sci. Total Environ. 712 (2020), 135759.

[12] Z.-Z. Zhang, Q.-Q. Zhang, Q. Guo, Q.-Q. Chen, X.-Y. Jiang, R.-C. Jin, Anaerobic ammonium-oxidizing bacteria gain antibiotic resistance during long-term acclimatization, Bioresour. Technol. 192 (2015) 756–764.

[13] I. Brook, Treatment of anaerobic infection, Expert Rev. Anti-infect. Ther. 5 (6) (2007) 991–1006.

[14] A. Ledezma, Y.-Y. Li, A. Wang, Biodegradability enhancement of wastewater containing cefalexin by means of the electro-Fenton oxidation process, J. Hazard. Mater. 227–228 (2012) 41–48.

[15] Q. Kong, Z.-B. Wang, L.i. Shu, M.-S. Miao, Characterization of the extracellular polymeric substances and microbial community of aerobic granulation sludge exposed to cefalexin, Int. Biodeterior. Biodegrad. 102 (2015) 375–382.

[16] L.-W. Meng, X.-K. Li, S.-T. Wang, L.-L. Liu, K.-L. Ma, J. Zhang, The long-term impact of cefalexin on organic substrate degradation and microbial community structure in EGSB system, Chemosphere 184 (2017) 215–223.

[17] A. Wagstaff, L.A. Lawton, B. Petrie, Polyamide microplastics in wastewater as vectors of cationic pharmaceutical drugs, Chemosphere 288 (2022), 132578.

[18] Y.-T. Zhang, W. Wei, Q.-S. Huang, C. Wang, Y. Wang, B.-J. Ni, Insights into the microbial response of anaerobic granular sludge during long-term exposure to polyethylene terephthalate microplastics, Water Res. 179 (2020), 115898.

[19] T. Gardon, C. Reisser, C. Soyez, V. Quillien, G. Le Moullac, Microplastics affect energy balance and gametogenesis in the pearl oyster pinctada margaritifera, Environ. Sci. Technol. 52 (9) (2018) 5277–5286.

[20] K. Liu, X. Wang, T. Fang, X.u. Pei, L. Zhu, D. Li, Source and potential risk assessment of suspended atmospheric microplastics in Shanghai, Sci. Total Environ. 675 (2019) 462–471.

[21] L. Tang, S.u. Chengyuan, Y.u. Chen, Y. Xian, X. Hui, Z. Ye, M. Chen, F. Zhu, H. e. Zhong, Influence of biodegradable polybutylene succinate and non-biodegradable polyvinyl chloride microplastics on anammox sludge: Performance evaluation, suppression effect and metagenomic analysis, J. Hazard. Mater. 401 (2021), 123337.

[22] W. Wei, X. Chen, L. Peng, Y. Liu, T. Bao, B.-J. Ni, The entering of polyethylene terephthalate microplastics into biological wastewater treatment system affects aerobic sludge digestion differently from their direct entering into sludge treatment system, Water Res. 190 (2021), 116731.

[23] Z. Wang, J. Gao, D. Li, H. Dai, Y. Zhao, Co-occurrence of microplastics and triclosan inhibited nitrification function and enriched antibiotic resistance genes in nitrifying sludge, J. Hazard. Mater. 399 (2020), 123049.

[24] H. Chen, M. Tang, X. Yang, Yiu Fai Tsang, Yanxin Wu, Dongbo Wang, Yaoyu Zhou, Polyamide 6 microplastics facilitate methane production during anaerobic digestion of waste activated sludge, Chem. Eng. J. 408 (2021), 127251.

[25] Y. Cui, J. Gao, D.a. Zhang, D. Li, H. Dai, Z. Wang, Y. Zhao, Responses of performance, antibiotic resistance genes and bacterial communities of partial nitrification system to polyamide microplastics, Bioresour. Technol. 341 (2021), 125767.

[26] X. Song, W.u. Xiaofeng, X. Song, C. Shi, Z. Zhang, Sorption and desorption of petroleum hydrocarbons on biodegradable and nondegradable microplastics, Chemosphere 273 (2021), 128553.

[27] V. Jalili, M. Ghanbari Kakavandi, A. Ghiasvand, A. Barkhordari, Masoud Ghanbari Kakavandi, Alireza Ghiasvand, Abdullah Barkhordari, Microextraction techniques for sampling and determination of polychlorinated biphenyls: A comprehensive review, Microchem. J. 179 (2022) 107442.

[28] Y. Mato, T. Isobe, H. Takada, H. Kanehiro, C. Ohtake, T. Kaminuma, Plastic resin pellets as a transport medium for toxic chemicals in the marine environment, Environ. Sci. Technol. 35 (2) (2001) 318–324.

[29] J. Martín, J.L. Santos, I. Aparicio, E. Alonso, Microplastics and associated emerging contaminants in the environment: Analysis, sorption mechanisms and effects of co-exposure, Trends Environ. Anal. Chem. 35 (2022) e00170.

[30] B. Fu, J. Luo, R. Xu, F. Fang, Q. Feng, T. Zhang, E. Yang, J. Cao, Co-impacts of the microplastic polyamide and sertraline on the denitrification function and microbial community structure in SBRs, Sci. Total Environ. 843 (2022), 156928.

[31] V. K. Kothari, 14 - Polyester and polyamide fibres – apparel applications, in: B.L. Deopura, R. Alagirusamy, M. Joshi, B. Gupta (Eds.) Polyesters and Polyamides, Woodhead Publishing2008, pp. 419-440.

[32] T. Matsuo, 17 - Automotive applications, in: B.L. Deopura, R. Alagirusamy, M. Joshi, B. Gupta (Eds.) Polyesters and Polyamides, Woodhead Publishing2008, pp. 525-541.

[33] Jing Sun, Xiaohu Dai, Qilin Wang, Mark C. M. Van Loosdrecht, Bing-Jie Ni, Microplastics in wastewater treatment plants: Detection, occurrence and removal, Water Research 152 (2019) 21-37.

[34] Y. Huang, W. Li, J. Gao, F. Wang, W. Yang, L.e. Han, D. Lin, B. Min, Y. Zhi, K. Grieger, J. Yao, Effect of microplastics on ecosystem functioning: Microbial nitrogen removal mediated by benthic invertebrates, Sci. Total Environ. 754 (2021), 142133.

[35] L. Wang, X. Li, Y. Wang, C. Wang, D. Ye, L. Zhou, H.u. Xue, Y. Ke, X.i. Xia, Determination of cephalexin residual level using ultra-high-performance liquid chromatography-tandem mass spectrometry: Residue depletion study in swine, J. Chromatogr. B 1124 (2019) 233–238.

[36] E. Danopoulos, M. Twiddy, R. West, J.M. Rotchell, A rapid review and meta-regression analyses of the toxicological impacts of microplastic exposure in human cells, J. Hazard. Mater. 427 (2022), 127861.

[37] M. Hesler, L. Aengenheister, B. Ellinger, R. Drexel, S. Straskraba, C. Jost, S. Wagner, F. Meier, H. Von Briesen, C. Büchel, P. Wick, T. Buerki-Thurnherr, Y. Kohl, Multi-endpoint toxicological assessment of polystyrene nano- and microparticles in different biological models in vitro, Toxicol. In Vitro 61 (2019), 104610.

[38] Q. Zhang, N.-S. Fan, F.u. Jin-Jin, B.-C. Huang, R.-C. Jin, Role and application of quorum sensing in anaerobic ammonium oxidation (anammox) process: A review, Crit. Rev. Environ. Sci. Technol. 51 (2020) 1–23.

[39] Z.-J. Shi, H.u. Hai-Yan, Y.-Y. Shen, X.u. Jia-Jia, M.-L. Shi, R.-C. Jin, Long-term effects of oxytetracycline (OTC) on the granule-based anammox: Process performance and occurrence of antibiotic resistance genes, Biochem. Eng. J. 127 (2017) 110–118.

[40] E.D. Traganza, Fluorescence excitation and emission spectra of dissolved organic matter in sea water, Bull. Mar. Sci. 19 (1969) 897–904.

[41] P.G. Coble, Coble, Characterization of marine and terrestrial DOM in seawater using excitation-emission matrix spectroscopy, Mar. Chem. 51 (4) (1996) 325–346.

[42] P. Coble, C. Castillo, B. Avril, Distribution and optical properties of CDOM in the Arabian Sea during the 1995 Southwest Monsoon, Deep Sea Res. Part II Top. Stud. Oceanogr. 45 (1998) (1995) 2195–2223.

[43] Z. Wang, Z. Wu, S. Tang, Characterization of dissolved organic matter in a submerged membrane bioreactor by using three-dimensional excitation and emission matrix fluorescence spectroscopy, Water Res. 43 (6) (2009) 1533–1540.

[44] C. Yin, F. Meng, G.-H. Chen, Spectroscopic characterization of extracellular polymeric substances from a mixed culture dominated by ammonia-oxidizing bacteria, Water Res. 68 (2015) 740–749.

[45] A.R. Badireddy, S. Chellam, P.L. Gassman, M.H. Engelhard, A.S. Lea, K.M. Rosso, Role of extracellular polymeric substances in bioflocculation of activated sludge microorganisms under glucose-controlled conditions, Water Res. 44 (15) (2010) 4505–4516.

[46] W. Wang, Y. Yan, Y. Zhao, Q. Shi, Y. Wang, Characterization of stratified EPS and their role in the initial adhesion of anammox consortia, Water Res. 169 (2020), 115223.

[47] J. Li, K. Zhang, H.a. Zhang, Adsorption of antibiotics on microplastics, Environ. Pollut. 237 (2018) 460–467.

[48] L. Zhou, T. Wang, G. Qu, H. Jia, L. Zhu, Probing the aging processes and mechanisms of microplastic under simulated multiple actions generated by discharge plasma, J. Hazard. Mater. 398 (2020), 122956.

[49] F. Wang, K.M. Shih, X.Y. Li, Kai Min Shih, Xiao Yan Li, The partition behavior of perfluorooctanesulfonate (PFOS) and perfluorooctanesulfonamide (FOSA) on microplastics, Chemosphere 119 (2015) 841–847.

[50] R.M. Razanajatovo, J. Ding, S. Zhang, H. Jiang, H. Zou, Sorption and desorption of selected pharmaceuticals by polyethylene microplastics, Mar. Pollut. Bull. 136 (2018) 516–523.

[51] X. Guo, C. Chen, J. Wang, Sorption of sulfamethoxazole onto six types of microplastics, Chemosphere 228 (2019) 300–308.

[52] Y. Yu, Y. Liu, L. Wu, Sorption and degradation of pharmaceuticals and personal care products (PPCPs) in soils, Environ. Sci. Pollut. Res. 20 (6) (2013) 4261–4267.

[53] T. Tennstedt, R. Szczepanowski, S. Braun, A. Pühler, A. Schlüter, Occurrence of integron-associated resistance gene cassettes located on antibiotic resistance plasmids isolated from a wastewater treatment plant, FEMS Microbiol. Ecol. 45 (2003) 239–252.

[54] Y. Zhao, S. Liu, B.o. Jiang, Y. Feng, T. Zhu, H. Tao, X.i. Tang, S. Liu, Genome-centered metagenomics analysis reveals the symbiotic organisms possessing ability

to cross-feed with anammox bacteria in anammox consortia, Environ. Sci. Technol. 52 (19) (2018) 11285–11296.
[55] L. Zhao, S.u. Chengyuan, W. Liu, R. Qin, L. Tang, X. Deng, W.u. Shumin, M. Chen, Exposure to polyamide 66 microplastic leads to effects performance and microbial community structure of aerobic granular sludge, Ecotoxicol. Environ. Saf. 190 (2020), 110070.
[56] Q. Zhang, J.-J. Fu, Q.-Y. Wu, J.-Y. Chen, N.-S. Fan, B.-C. Huang, R.-C. Jin, Build the expressway for the salt-tolerant anammox process: Acclimation strategy tells the story, J. Cleaner Prod. 278 (2021) 123921.
[57] D. Wang, T. Li, K. Huang, X. He, X.-X. Zhang, Roles and correlations of functional bacteria and genes in the start-up of simultaneous anammox and denitrification system for enhanced nitrogen removal, Sci. Total Environ. 655 (2019) 1355–1363.
[58] D.a. Kang, Y.u. Tao, X.u. Dongdong, Z. Zeng, A. Ding, M. Zhang, S. Shan, W. Zhang, P. Zheng, The anammox process at typical feast-famine states: Reactor performance, sludge activity and microbial community, Chem. Eng. J. 370 (2019) 110–119.
[59] S.-J. Chun, Y.-J. Kim, Y. Cui, K.-H. Nam, Ecological network analysis reveals distinctive microbial modules associated with heavy metal contamination of abandoned mine soils in Korea, Environ. Pollut. 289 (2021), 117851.
[60] C. Wang, S. Liu, X.u. Xiaochen, C. Zhang, D. Wang, F. Yang, Achieving mainstream nitrogen removal through simultaneous partial nitrification, anammox and denitrification process in an integrated fixed film activated sludge reactor, Chemosphere 203 (2018) 457–466.
[61] M. Tosin, A. Pischedda, F. Degli-Innocenti, Biodegradation kinetics in soil of a multi-constituent biodegradable plastic, Polym. Degrad. Stab. 166 (2019) 213–218.
[62] K.-Y. Law, Definitions for hydrophilicity, hydrophobicity, and superhydrophobicity: getting the basics right, J. Phys. Chem. Lett. 5 (2014) 686–688.
[63] M. Bouhedda, S. Lefnaoui, S. Rebouh, M.M. Yahoum, Predictive model based on Adaptive Neuro-Fuzzy Inference System for estimation of Cephalexin adsorption on the Octenyl Succinic Anhydride starch, Chemomet. Intell. Lab. Syst. 193 (2019), 103843.
[64] Y. Xiong, J. Zhao, L. Li, Y. Wang, X. Dai, Y.u. Fei, J. Ma, Interfacial interaction between micro/nanoplastics and typical PPCPs and nanoplastics removal via electrosorption from an aqueous solution, Water Res. 184 (2020), 116100.
[65] G. Liu, Z. Zhu, Y. Yang, Y. Sun, Y.u. Fei, J. Ma, Sorption behavior and mechanism of hydrophilic organic chemicals to virgin and aged microplastics in freshwater and seawater, Environ. Pollut. 246 (2019) 26–33.
[66] L. Zhao, L. Rong, X.u. Jiaping, J. Lian, L. Wang, H. Sun, Sorption of five organic compounds by polar and nonpolar microplastics, Chemosphere 257 (2020), 127206.
[67] L.Z. Lara, C. Bertoldi, N.M. Alves, A.N. Fernandes, Crislaine Bertoldi, Nortom Munhoz Alves, Andreia Neves Fernandes, Sorption of endocrine disrupting compounds onto polyamide microplastics under different environmental conditions: Behaviour and mechanism, Sci. Total Environ. 796 (2021) 148983.
[68] X. Ji, W.u. Zhuoying, S. Sung, P.-H. Lee, Metagenomics and metatranscriptomics analyses reveal oxygen detoxification and mixotrophic potentials of an enriched anammox culture in a continuous stirred-tank reactor, Water Res. 166 (2019), 115039.
[69] S. Yanase, K. Yasuda, N. Ishii, Interaction between the ins/IGF-1 and p38 MAPK signaling pathways in molecular compensation of sod genes and modulation related to intracellular ROS levels in C. elegans, Biochem. Biophys. Rep. 23 (2020), 100796.
[70] F.u. Jinjin, Q. Zhang, B. Huang, N. Fan, R. Jin, A review on anammox process for the treatment of antibiotic-containing wastewater: Linking effects with corresponding mechanisms, Front. Environ. Sci. Eng. 15 (2020) 17.
[71] K. Zhuang, D. Shi, Z. Hu, F. Xu, Y. Chen, Z. Shen, Subcellular accumulation and source of O2− and H2O2 in submerged plant Hydrilla verticillata (L.f.) Royle under NH4+-N stress condition, Aquat. Toxicol. 207 (2019) 1–12.